

Enhanced light emission of $\text{In}_x\text{Ga}_{1-x}\text{As}$ quantum dots in a two-dimensional photonic-crystal defect microcavity

T. D. Happ,* I. I. Tartakovskii,† V. D. Kulakovskii,‡ J.-P. Reithmaier, M. Kamp, and A. Forchel
Technische Physik, University of Würzburg, Am Hubland, 97074 Würzburg, Germany

(Received 20 November 2001; revised manuscript received 11 February 2002; published 16 July 2002)

The interaction of self-assembled $\text{In}_x\text{Ga}_{1-x}\text{As}$ quantum dots with nondegenerate modes of a two-dimensional photonic-crystal defect microcavity has been investigated in the weak-coupling regime. Photoluminescence intensity measurements show a transition from a pump rate limited regime at low excitation to cavity-controlled modes at high excitation. We observe considerably different saturation levels for quantum dots on and off the defect resonance. An enhancement of light emission by a factor of 9 due to the Purcell effect is obtained from this saturation behavior. Using the different temperature shifts of the quantum dot emission lines and the cavity mode, individual dots are tuned in and out of resonance, thus controlling their spontaneous emission rate.

DOI: 10.1103/PhysRevB.66.041303

PACS number(s): 42.70.Qs, 42.79.Gn, 12.20.-m

Since its prediction by Purcell¹ and early work in the microwave domain using atoms in resonators,² tailoring of spontaneous emission (SE) at optical frequencies is an area of intense research. Progress in microfabrication technologies and the use of self-assembled semiconductor quantum dots (QDs) as atomlike emitters with a discrete set of states made possible a realization of cavity-quantum electrodynamics (C-QED) experiments in solid-state systems.³⁻⁶ Besides giving insight in fundamental problems regarding the interaction of light and matter, this work leads to highly interesting potential applications, ranging from high-speed light sources to quantum information processing and quantum cryptography.^{7,8} The key to SE control is a classical C-QED experiment, where an atomlike two-level emitter is placed in a high finesse cavity. In the weak-coupling regime, its physics are governed by the Purcell effect, where the spontaneous emission rate of an emitter on-resonance with a cavity mode is enhanced, while off-resonance emission is suppressed. For strong-coupling SE becomes reversible and the resonance energies are changed, which is known as Rabi splitting.⁹ The magnitude of SE enhancement in the weak-coupling case is described by the Purcell factor $F_p = (3/4\pi^2)(\lambda/n)^3 Q/V_m$ for an emitter located in a field maximum, where λ is the wavelength and n the refractive index of the cavity with quality factor Q and mode volume V_m . For the experimental realization it is therefore necessary to achieve high Q -factors and small mode volumes. Using for example semiconductor microdiscs or pillar microcavities, both enhancement on-resonance and SE suppression off-resonance was demonstrated.^{3-5,10}

A different approach is the use of photonic-crystal (PC) defect microcavities,¹¹ where the cavity volume is reduced so far that most of the modes are cut off. Defect microcavities were predicted to offer high Q -factors in conjunction with very small mode volumes and are therefore particularly promising for the realization of pronounced C-QED effects.^{12,13} So far, only the spectroscopy of cavity modes at high excitation was reported for such PC defect cavities with QD light emitters.¹⁴⁻¹⁷

We present the spectroscopic characterization of a hexagonal defect microcavity (“ $H2$ ”) formed in a waveguide-

based two-dimensional (2D) PC. The observed mode structure with Q -factors up to 800 is matched with the theoretically expected eigenmodes of the defect cavity. Excitation power-dependent measurements show a transition from a pump rate limited regime to a cavity resonance-controlled regime with different saturation behavior for QDs on- and off-resonance. It is possible to estimate a $\times 9$ SE rate enhancement due to the Purcell effect. Using temperature tuning of the QD emission wavelength it is possible to bring individual QDs into resonance with the cavity mode and thus control their SE rate.

The PC microcavities are fabricated on a GaAs/ $\text{Al}_x\text{Ga}_{1-x}\text{As}$ heterostructure grown by molecular beam epitaxy on a (100) GaAs substrate. It consists of 460 nm $\text{Al}_{0.9}\text{Ga}_{0.1}\text{As}$ as lower cladding layer, a 215 nm thick GaAs waveguide containing a single layer of self-assembled $\text{In}_x\text{Ga}_{1-x}\text{As}$ QDs followed by a 310 nm $\text{Al}_{0.2}\text{Ga}_{0.8}\text{As}$ upper cladding and a 20 nm GaAs protection layer. The QD layer has a dot density of $3 \times 10^{10} \text{ cm}^{-2}$ and shows a broad photoluminescence (PL) spectrum around $E = 1.25\text{-}1.34 \text{ eV}$ at low temperatures due to QD size fluctuations and the resulting strong inhomogeneous broadening. At high excitation the emission is extended to $E = 1.38 \text{ eV}$ due to contributions from higher excited QD states.

A triangular PC dot pattern with a lattice period of $a = 290 \text{ nm}$ and air fill factor $f = (2\pi/\sqrt{3})(r/a)^2 \cong 40\%$ is defined using 100 kV electron-beam lithography. The hexagonal defect is created by seven missing holes in the center of an otherwise unperturbed $20 \mu\text{m}$ large PC field. This PC pattern is etched into the semiconductor using a dielectric etch mask in conjunction with a highly anisotropic Cl_2/Ar chemically assisted ion beam etch process. The etched holes are 850 nm deep. This results in a 99.9% overlap of the intensity distribution of the planar index waveguide mode with the PC, which is necessary to minimize radiation losses into the substrate and makes possible the fabrication of high Q cavities.¹⁸

We are using a micro-PL setup with independent spatial resolution for excitation and detection perpendicular to the plane of the 2D PC. This allows the investigation of the

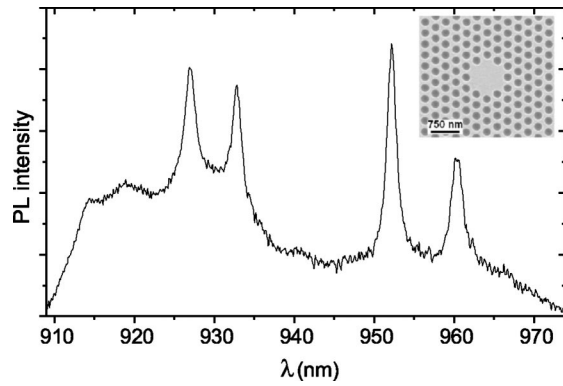


FIG. 1. PC defect cavity spectrum at $T=40$ K and 5.7 kW/cm² excitation power density. Inset: top view SEM micrograph of the photonic-crystal microcavity with $a=290$ nm lattice constant and $r=0.33$ a hole radius.

in-plane cavity modes using the light leaking from the waveguide structure mainly due to scattering and diffraction in the patterned area. The sample is cooled to temperatures of 30 K to 70 K in a He-flow cryostat and optically excited with a continuous wave Ar⁺ laser at 514.5 nm. The pump beam is focused on the sample through a large working-distance microscope objective ($NA=0.4$) mounted outside the cryostat, resulting in a spot size of 3 μ m diameter. The emitted PL light is collected with the same objective and focused with an additional lens to an intermediate plane equipped with adjustable crossed slits, providing a spatial resolution of 2 μ m. The selected PL is analyzed by a spectrometer (0.46 m, 300 mm⁻¹ grating) equipped with a cooled Si charge-coupled device (CCD) camera.

Figure 1 shows an unprocessed spectrum as obtained from the defect cavity at $T=40$ K and 5.7 kW/cm² excitation power density. It exhibits four pronounced lines on top of a broad background. The sharp lines, a pair at 927 nm and 933 nm wavelength and a second pair at 952 nm and 960 nm, are identified as four of the defect modes of the $H2$ cavity. The Q -factors of the modes range from 550 to 800, as extracted from a fit of Lorentz profiles. They are only observed when both excitation spot and detection area are tightly focused on the defect. This is consistent with the strongly localized nature of these cavity modes.

We have obtained the cavity eigenmode spectrum from numerical 2D calculations using a block-iterative frequency-domain method.¹⁹ A $H2$ cavity with 40% air fill factor and an effective refractive index of 3.28 supports 18 modes which are distributed over the whole TE-polarized ($\vec{E} \perp$ holes) photonic bandgap region. As this TE photonic band gap extends from normalized frequencies of $u=a/\lambda=0.227$ - 0.320 , only six of the cavity modes are within the bandwidth of the QD PL. The theoretical calculation for a perfectly symmetric PC predicts twofold degenerate modes at $u=0.303$, 0.312 , and 0.318 , respectively. In the experiment, structural fluctuations in the PC lift the degeneracy and cause a splitting of the modes. We therefore attribute the modes observed at $u=0.302$ and 0.305 to the split degenerate mode at $u=0.303$, which shows electric field distributions similar to Fabry-Perot modes with two additional lat-

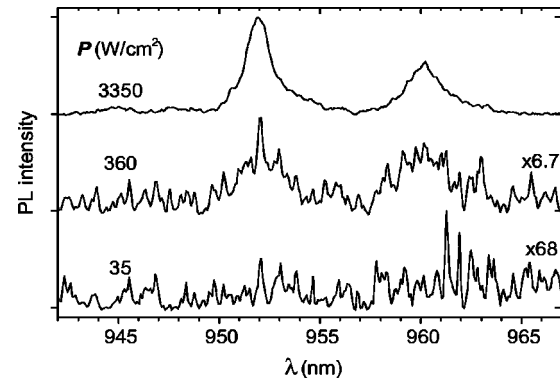


FIG. 2. Excitation power dependence of the QD photoluminescence in the region of the longer wavelength cavity modes at $T=30$ K. The background subtracted spectra are vertically shifted and normalized by the indicated factors.

eral nodes. The shorter wavelength mode pair at $u=0.311$ and 0.313 can be assigned to the degenerate mode at $u=0.312$ while the additional, weaker features in the spectrum at 914 nm and 919 nm wavelength correspond to the highest frequency defect modes at $u=0.318$. As their spectral position is already very close to the edge of the band gap, they are not as strongly localized as their counterparts lying deeper in the photonic band gap. Therefore, their Q -factor is much lower and they are only weakly resolved.

As only the PL in the region of the two longest wavelength peaks stems exclusively from ground-state transitions of the QDs, we will focus on these two modes for the further analysis. In Fig. 2, normalized and background subtracted spectra of this region obtained at different excitation power are displayed. At the lowest pump power, many sharp lines are visible. Surprisingly, there is no indication of cavity modes. These only emerge at higher pumping levels and are fully visible only at high excitation, while the sharp lines can be no longer resolved.

These sharp lines are due to ground-state transitions of individual QDs in the defect cavity. The number of individual lines across the inhomogeneous distribution agrees well with the estimated 170 QDs in the cavity. The fact that the cavity modes are not visible is due to the low pump power: The spontaneous emission rate of the QDs is limited by the pump rate with which new carriers are generated and captured in the QDs. In this regime, no discrimination between on- and off-resonance QDs is possible, as the spontaneous emission lifetime of even QDs off-resonance is shorter than the time between two successive carrier capture events. At higher pump power, carriers are already generated at a rate which allows a higher spontaneous emission rate for QDs on-resonance with the cavity modes, so that the mode peaks emerge from the spectra. The lines of the individual QD transitions are still visible, but they suffer an additional homogeneous broadening due to the quantum confined Stark effect. With increasing excitation power the increasing charge density fluctuates in the vicinity of a QD, resulting in fluctuating single-dot line positions.²⁰ This is most pronounced at the highest pump power, where the individual QD lines are no longer resolved. Here the charge generation

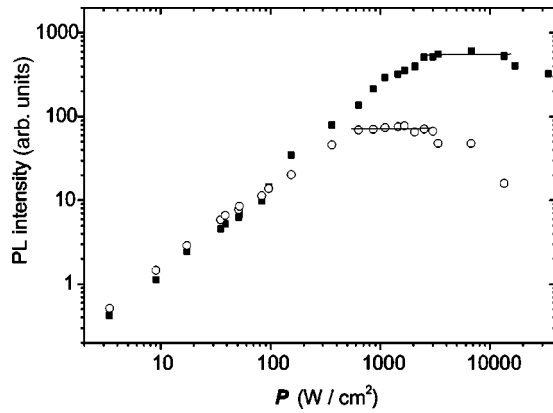


FIG. 3. Excitation power dependence of the PL intensity at $T = 30$ K from an ensemble of QDs on-resonance (solid squares, $\lambda = 951.8\text{--}953.1$ nm) and off-resonance (open circles, $\lambda = 942.0\text{--}945.9$ nm) with the cavity mode. The lines are linear fits to the saturation regimes.

rate is high enough so that the intensity of spontaneous emission of the QDs is determined by their individual spontaneous emission lifetime, as determined by the magnitude of the Purcell effect. Consequently, the cavity modes are most pronounced under these excitation conditions.

A more detailed analysis of this evolution of PL with excitation power density is presented in Fig. 3: Here we plot the integrated PL intensity from a QD ensemble on resonance with the cavity mode ($\lambda = 951.8\text{--}953.1$ nm, solid squares) compared to an off-resonance reference region ($\lambda = 942.0\text{--}945.9$ nm, open circles). In the low power-density regime up to about 100 W/cm^2 , the QD PL from the mode and the reference region cannot be distinguished. Both exhibit a linear increase with pump power. This indicates that here the emission rate of the QDs is limited by the carrier generation rate as determined by pump power rather than the spontaneous emission lifetime of the individual QD. At intermediate excitation power ($150\text{--}600\text{ W/cm}^2$) the QDs on resonance have a higher PL intensity compared to the off-resonance QDs, but still intensity grows linearly. This indicates that due to different radiative lifetimes for on- and off-resonance QDs, the generated carriers are already distributed differently among the QDs, but the overall emission rate is still limited by the pump power. At higher excitation levels the PL of QDs off-resonance clearly saturates first due to the filling of the fundamental QD states. Here the emission rate is determined by the radiative lifetime of these QDs. In contrast, for the QDs on-resonance the PL intensity further increases linearly, until it finally saturates at a $10\times$ higher level. This shows that the on-resonance QDs are less subject to state filling, or, in other words, have a higher spontaneous emission rate due to the Purcell effect.¹⁰ At even higher pump powers the intensity decreases again, as here the carrier density no longer grows linearly with pump power, but instead additional loss channels such as Auger effects or lattice heating are introduced.

From the differences in PL saturation behavior on- and off-resonance which were observed for several similar samples, it is possible to estimate the magnitude of the Pur-

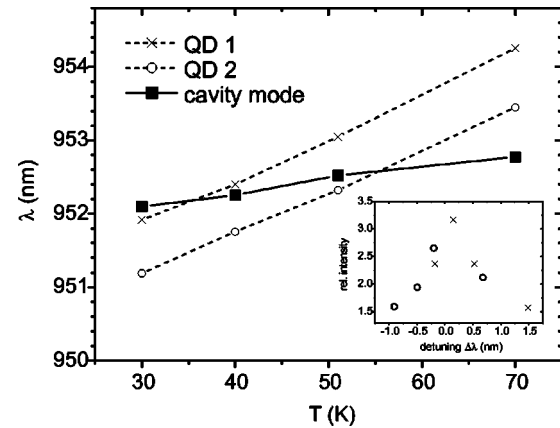


FIG. 4. Temperature shift of the dominant cavity mode obtained at high-excitation power density compared to two individual QD lines obtained at low excitation power density. Inset: PL intensity of the two QDs at intermediate-excitation power depending on the detuning to the cavity mode.

cell effect. This is valid, as stimulated emission can be neglected for the investigated structures.²¹ In order to account for the different number of QDs and to eliminate possible differences in PL extraction efficiency for on- and off-resonance QDs, we first normalize the PL intensity to equal values in the regime of linear growth at low excitation power. Then the PL intensity levels in saturation I_{on} , I_{off} reflect the spontaneous emission rate into both the cavity mode and leaky modes for on-resonance QDs, and solely into the leaky modes for off-resonance QDs.⁴ Therefore, in order to extract the relative emission rate into the cavity mode, it is necessary to calculate the normalized difference of the PL intensities $(I_{on} - I_{off})/I_{off}$ in saturation. This yields a SE enhancement factor of 9. The theoretically expected Purcell factor for the cavity mode volume of $V_m = 17.5 (\lambda/2n)^3$ and $Q = 680$ is $F_p = 19$ for the ideal case with all QDs located at the field intensity maximum of the cavity mode. Assuming only negligible suppression of the off-resonance SE due to the coupling to leaky modes, it is valid to compare this SE enhancement factor to F_p . Due to the random dot distribution in the cavity, a lower value for the spontaneous emission enhancement is expected in the experiment.³ This is in good agreement with the data.

In addition to the study of the collective behavior of an ensemble of QDs in the cavity, it is also possible to investigate the interaction of a single QD with the cavity mode. For this it is necessary to observe both individual QD lines and the cavity mode simultaneously, as is possible at intermediate pump levels. Using the different wavelength shifts⁵ of the QD emission and of the cavity mode with temperature, it is possible to tune individual QDs in and out of resonance. An example is displayed in Fig. 4. Tracing the PL intensity of the QD lines as they are tuned across the mode allows a direct observation of the emission rate enhancement. For this experiment the QD PL intensity at each temperature was normalized with respect to a reference dot ($\lambda = 955.3$ nm) with large detuning to the cavity mode. This eliminates fluctuations due to slightly varying excitation conditions arising from thermal expansion of the cryostat. The QD intensity

depending on the detuning from the cavity mode is displayed in the inset of Fig. 4. The intensity maximum around zero detuning is clearly visible. However, the absolute magnitude of the intensity enhancement is much smaller than the value observed from the QD ensemble. The reason for this is the lower excitation power used in this experiment, which is necessary to resolve the individual QD lines. As neither the QDs on- nor off-resonance are in saturation, the overall emission rate is limited by the excitation power. Therefore it is not possible to observe the full magnitude of the Purcell effect for individual QDs in the temperature-dependent experiment.

In summary, we have studied the interaction of self-assembled $\text{In}_x\text{Ga}_{1-x}\text{As}$ quantum dots with a hexagonal 2D PC defect microcavity in the weak-coupling regime. Nondegenerate cavity modes with Q -factors up to 800 could be identified using numerical eigenmode calculations. Pump

power-dependent PL measurements show the transition from a pump rate limited regime with undistinguishable QDs on- and off-resonance to the lifetime-limited regime with different saturation levels for the QDs on- and off-resonance. Taking into account the coupling of the QDs to both cavity mode and leaky modes, a ninefold enhancement of the spontaneous emission rate for QDs on-resonance was estimated. In addition, individual QDs were tuned in and out of resonance with the cavity, thus controlling their spontaneous emission rate.

The authors would like to thank F. Klopff and K. Avary for expert sample growth and etching, Nanosystems and Technologies GmbH for SiO_2 coating, and M. Bayer for fruitful discussions. The financial support by DARPA under the QuIST program and by the State of Bavaria is gratefully acknowledged.

*Electronic address: happ@physik.uni-wuerzburg.de

[†]On leave from Institute of Solid State Physics, Russian Academy of Science, 142432 Chernogolovka, Russia.

¹E.M. Purcell, Phys. Rev. **69**, 681 (1946).

²R.G. Hulet, E.S. Hilfer, and D. Kleppner, Phys. Rev. Lett. **55**, 2137 (1985).

³J.M. Gérard *et al.*, Phys. Rev. Lett. **81**, 1110 (1998).

⁴M. Bayer *et al.*, Phys. Rev. Lett. **86**, 3168 (2001).

⁵A. Kiraz *et al.*, Appl. Phys. Lett. **78**, 3932 (2001).

⁶G.S. Solomon, M. Pelton, and Y. Yamamoto, Phys. Rev. Lett. **86**, 3903 (2001).

⁷A. Imamoglu *et al.*, Phys. Rev. Lett. **83**, 4204 (1999).

⁸P. Michler *et al.*, Science **290**, 2282 (2000).

⁹L.C. Andreani, G. Panzarini, and J.-M. Gérard, Phys. Rev. B **60**, 13 276 (1999).

¹⁰B. Gayral and J.-M. Gérard, Physica E (Amsterdam) **7**, 641 (2000).

¹¹R.D. Meade *et al.*, Phys. Rev. B **44**, 13 772 (1991).

¹²O. Painter, J. Vučković, and A. Scherer, J. Opt. Soc. Am. B **16**, 275 (1999).

¹³R. Coccioli *et al.*, IEE Proc. Optoelectron. **145**, 391 (1998).

¹⁴C.J.M. Smith *et al.*, Electron. Lett. **35**, 228 (1999).

¹⁵C.J.M. Smith *et al.*, J. Opt. Soc. Am. B **17**, 2043 (2000).

¹⁶C. Reese *et al.*, Appl. Phys. Lett. **78**, 2279 (2001).

¹⁷T. Yoshie *et al.*, Appl. Phys. Lett. **79**, 114 (2001).

¹⁸B. D'Urso *et al.*, J. Opt. Soc. Am. B **15**, 1155 (1998).

¹⁹S.G. Johnson and J.D. Joannopoulos, Opt. Express **8**, 173 (2001).

²⁰W. Heller, U. Bockelmann, and G. Abstreiter, Phys. Rev. B **57**, 6270 (1998).

²¹An estimation of the mean photon number in the cavity gives negligible stimulated emission: There are ~ 10 QDs emitting in the mode with an average radiative lifetime of 110 ps ($\tau = 1$ ns, $F_p = 9$) and a photon lifetime of 2 ps ($Q = 680$, $\lambda = 952$ nm). This gives an average photon number of $10 \times \frac{2}{110} = 0.18$ and, using Poisson statistics, a probability of 1.4% for finding more than one photon at a time.